Single-Qubit Error Mitigation by Simulating Non-Markovian Dynamics

Mirko Rossini, Dominik Maile, Joachim Ankerhold, and Brecht I. C. Donvil*
Institute for Complex Quantum Systems and IQST, Ulm University—Albert-Einstein-Allee 11, D-89069 Ulm, Germany

(Received 6 March 2023; revised 9 June 2023; accepted 16 August 2023; published 15 September 2023)

Quantum simulation is a powerful tool to study the properties of quantum systems. The dynamics of open quantum systems are often described by completely positive (*CP*) maps, for which several quantum simulation schemes exist. Such maps, however, represent only a subset of a larger class of maps: the general dynamical maps which are linear, Hermitian preserving, and trace preserving but not necessarily positivity preserving. Here we present a simulation scheme for these general dynamical maps, which occur when the underlying system-reservoir model undergoes entangling (and thus non-Markovian) dynamics. Such maps also arise as the inverse of *CP* maps, which are commonly used in error mitigation. We illustrate our simulation scheme on an IBM quantum processor, demonstrating its ability to recover the initial state of a Lindblad evolution. This paves the way for a novel form of quantum error mitigation. Our scheme only requires one ancilla qubit as an overhead and a small number of one and two qubit gates. Consequently, we expect it to be of practical use in near-term quantum devices.

DOI: 10.1103/PhysRevLett.131.110603

Introduction.—Quantum computing has created a computational paradigm that may lead to the development of new and powerful solutions to computational tasks. A prominent application of digital quantum computers is their ability to simulate other quantum systems, particularly at the level of noisy intermediate scale (NISQ) quantum platforms [1].

Although there exists a range of quantum simulation methods for closed quantum systems, see, e.g., [2–5], the simulation of an open quantum system is more arduous. Since it is often not possible to simulate the complete system-environment joint dynamics, simulation methods instead focus on realizing the effective reduced dynamics of the open quantum system alone.

In the case that one assumes that system and environment are initially in a product state, the evolution is guaranteed to be described by a completely positive (*CP*) map [6] acting on the initial system state, which can be obtained via numerical methods ([7–11]) and perturbative schemes [12]. A *CP* map is said to be *CP* divisible if it can be subdivided into maps that are themselves *CP*. In such a scenario, the evolution of the system may be described by the Lindblad-Gorini-Kossakowski-Sudarshan equation [13,14]. If, however, the system-environment amalgam accumulates significant correlations, the evolution is non-Markovian and *CP* maps no longer provide an appropriate description [15].

Quantum simulation methods for Lindblad-like dynamics have been extensively studied [16–23] and experimentally implemented [24]. An efficient simulation scheme for any qubit *CP* map was developed by [25], based on results of [26,27]. Other methods are [28,29] and collision models [30,31], which are able to simulate non-Markovian dynamics [32–35].

In the current NISQ era, quantum error mitigation forms an important set of strategies to deal with noise [36]. One such strategy relies on the assumption that the dominant effect of noise on a quantum system can be modeled via a *CP* map. The goal is then to apply the inverse of this noise map to that system in order to arrive at its "undisturbed" state from which expectation values are computed. This way, the impact of noise is mitigated while residual system-reservoir correlations may still be present. In general, the inverse of a *CP* map cannot be directly implemented on a quantum processor, but it can be represented by a quasi-probability distribution (a probability distribution that can take negative values) of *CP* maps. Realizing this quasi-probability distribution is the essence of the error mitigation method proposed in [37–41] such that on average expectation values of the undisturbed state are obtained. One of the challenges is to find an efficient way to realize the *CP* maps that represent the inverse.

In this Letter we propose a novel simulation scheme for general qubit dynamical maps which extends beyond *CP* divisible maps [25–27]. General dynamical maps are trace preserving and Hermiticity preserving, but not necessarily positivity preserving. They naturally arise as the inverse of *CP* maps, and thus allow for error mitigation. In Fig. 1 we recover several initial states of a qubit disturbed by a thermal Lindblad equation on an IBM quantum processor. General dynamical maps also arise as the solutions of general time-local master equations, i.e., master equations beyond the Lindblad form. Their derivation is based on tracing the environment in Gaussian [42–46] or other

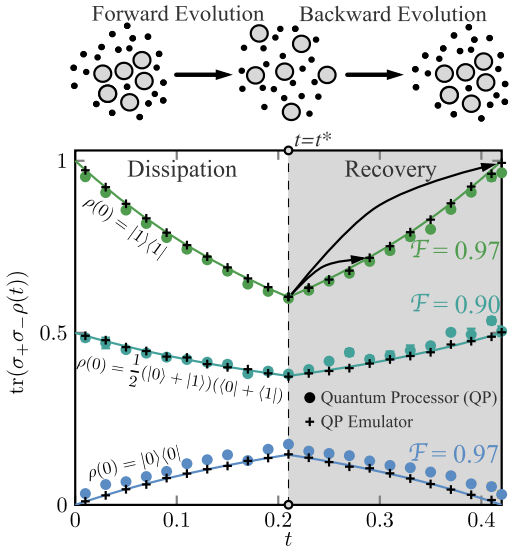

FIG. 1. (Top) Reversing the direction of time in a dissipative system brings it back to its initial state. (Bottom) We recover the initial state of a Lindblad evolution (6) by simulating its time-reversed evolution $(d/dt)\rho_t = -\mathcal{L}_t(\rho_t)$. For $t \le t^*$ the points show the forward evolution simulated on an IBM quantum computer, while for $t > t^*$ they denote the reverse evolution. The lines represent the numerical to both Eq. (6) and its time-reversed equivalent. $\mathcal{F}$ gives the fidelity between the final recovered state and the initial state. The parameters of these master equations are $\beta = \omega = \gamma = 1$.

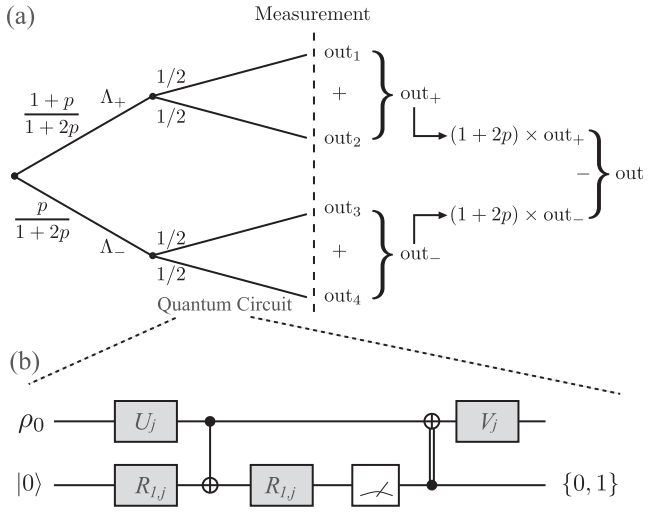

FIG. 2. (a) Representation of the algorithm simulating general dynamical maps decomposed as the weighted difference of two CPTP maps 4. At each branching point a choice is made with a classical random number generator (weighted with the indicated probabilities). At the dashed line, the measurement of some observable is performed. Finally, the outcomes are rescaled and subtracted from one another. (b) The circuit employed in [25] to realize the extremal maps (2).

exactly solvable models [47], or via time convolutionless perturbation theory [12,48].

We exploit the fact that general dynamical maps acting on finite dimensional systems can always be decomposed as the difference of two *CP* maps [49,50]. We demonstrate that this decomposition can be brought into a suitable form for quantum simulations, namely, as a weighted difference of two completely positive trace-preserving (CPTP) maps. Combining this result with the work of [25–27], our simulation scheme provides an efficient manner to implement the error mitigation described in [37–39].

The main advantage of the algorithm we present here is its problem-agnostic applicability. No specific design is required for the dynamics one aims to simulate. In fact, we are able to simulate the dynamics of a given system from any point in time to any later time. As an additional benefit, our proposed scheme is resource efficient as the depth of the quantum circuit proposed by [25] does not grow with the simulated time. We illustrate these features by implementing two examples on IBM quantum processors, which demonstrate the ability to simulate the time evolution from any intermediate point in time, regardless of whether the evolution map is *CP* and the ability to recover the initial state of a Lindbladian evolution [51], see Fig. 1.

Theoretical framework.—A finite dimensional linear map Λ is *CP* if and only if its action on a state ρ can be written in terms of a set of matrices $\{K_j\}_j$, often referred to as Kraus operators: $\Lambda(\rho) = \sum_j K_j \rho K_j^\dagger$. The map is trace preserving if and only if $\sum_j K_j^\dagger K_j = \mathbb{I}$, where $\mathbb{I}$ is the identity on the appropriate Hilbert space, see, e.g., [6,12]. The results of [26,27] prove that any CPTP map Λ for *qubits* is equal to the convex sum of two extremal *CP* maps Λ_1 and Λ_2, which may in turn be realized by a pair of Kraus operators. Concretely, they showed that for every CPTP qubit map Λ, there exist two pairs of unitaries U_j, V_j and two pairs of Kraus operators $F_{i,j}$ (with $i, j \in \{1, 2\}$) defining the extremal maps

$$\Lambda_j(\rho) = V_j\left(\sum_{i=1}^{2} F_{i,j}(U_j \rho U_j^\dagger)F_{i,j}^\dagger\right)V_j^\dagger, \tag{1}$$

such that

$$\Lambda(\rho) = \frac{1}{2}\Lambda_1(\rho) + \frac{1}{2}\Lambda_2(\rho). \tag{2}$$

The authors of [25] devised a simple circuit shown in Fig. 2(b) to realize the action of the Λ_j using just one ancillary qubit and CNOT gates.

General dynamical maps are linear, trace, and Hermiticity preserving but not necessarily positivity preserving. For finite-dimensional systems such maps can always be written as the difference of two *CP* maps [50]

$$\Sigma(\rho) = \Lambda_+(\rho) - \Lambda_-(\rho) = \sum_j K_j \rho K_j^\dagger - \sum_j M_j \rho M_j^\dagger; \tag{3}$$

see Supplemental Material [50] for more details on how to derive this decomposition, which includes Refs. [52,53]. The map Σ is trace preserving if and only if $\sum_j K_j^\dagger K_j - \sum_j M_j^\dagger M_j = \mathbb{I}$. Since $\Lambda_\pm$ are bounded, there exists a positive number p such that $\sum_j M_j^\dagger M_j \leq p\mathbb{I}$. We define the semi-positive definite operator $D = \sqrt{p\mathbb{I} - \sum_j M_j^\dagger M_j}$ and write

$$\Sigma(\rho) = (1+p)\Lambda_+^* - p\Lambda_-^*, \tag{4}$$

where $\Lambda_+^* = [(\sum_j K_j \rho K_j^\dagger + D\rho D^\dagger)/(1+p)]$ and $\Lambda_-^* = [(\sum_j M_j \rho M_j^\dagger + D\rho D^\dagger)/(p)]$. It is straightforward to check that both maps $\Lambda_\pm^*$ are trace preserving and CP. The above equation is our first main result. It shows that any general dynamical map Σ can be decomposed as the weighted difference of two CPTP maps. The above decomposition is an alternative to the decomposition in terms of CPTP maps by [54] which involves applying positive, nonunitary transformations to the quantum state. The latter makes our decomposition more attuned for simulating the action of Σ on an experimental platform.

Algorithm and circuit schemes.—Our simulation scheme for general dynamical maps is illustrated in Fig. 2(a). First, a classical random number generator is used to choose the branch Λ_+^* or Λ_-^* corresponding to Eq. (4), with probabilities $(1+p)/(1+2p)$ and $[p/(1+2p)]$, respectively. Then one of the two extremal maps (2) is selected with probability $1/2$ and realized by the circuit representation of [25], as shown in Fig. 2(b). Next, an observable is measured and the outcomes within the plus and minus branch are summed. Finally, the measurement result is rescaled by $1+2p$ to restore normalization, and the results of both branches are subtracted.

The scheme depicted in Fig. 2 can be straightforwardly implemented on a quantum computational platform [55]. Generating the dynamics of a system using the algorithm described above requires eight different quantum circuits of the type shown in Fig. 2(b). Each circuit requires single-qubit unitary gates U_j, V_j, $R_{1,j}$, and $R_{2,j}$, which we construct explicitly in [50], and are realized via a universal set of single-qubit gates. Beyond single-qubit unitary gates, CNOT gates and a measurement operation on the ancilla are implemented. With this circuit representation any single qubit map Σ can be simulated with an error $\leq \varepsilon$ using a quantum computer time of $O[\mathrm{polylog}(1/\varepsilon)]$ [25].

We will first demonstrate that our scheme allows us to simulate general dynamical maps and then use it for error mitigation on an actual quantum computing device [53]. For optimal performance, qubits and connections with the least error rate are selected for each circuit implementation and specific gate protocols are optimized to minimize the number of CX gates. An initial exploratory run on the device uncovers its systematic readout error, later used to correct measurement results [50]. Each data point in Figs. 1 and 4 is averaged over ten runs of 10 000 shots each, i.e., 10 000 circuits are implemented according to the probability distribution in Fig. 2(a). Error bars are within the size of the data points. The final infidelity is mostly due to systematic errors in the quantum gates and measurement scheme within a specific circuit calibration [56].

Simulating general time local master equations.—General trace-preserving time-local master equations are of the form

$$\begin{aligned}\frac{d}{dt}\rho_t &= \mathcal{L}_t(\rho_t) \\ &= -i[H(t),\rho_t] + \sum_k \Gamma_k(t)\left(L_k\rho_t L_k^\dagger - \frac{1}{2}\{L_k^\dagger L_k,\rho_t\}\right),\end{aligned} \tag{5}$$

where the L_k are operators and the $\Gamma_k(t)$ scalar weight functions.

The above equation has the appearance of a Lindblad equation with the exception that its weight functions $\Gamma_k(t)$ are not assumed to be positive definite. General time-local master equations describe the evolution of a wide class of open quantum systems, as they can be derived from the Nakajima-Zwanzig equation [57] when its solution has an inverse that exists over a finite time interval [58–62]. For an initial condition ρ_0 the formal solution of Eq. (5) is $\rho_t = \Lambda_{t,0}(\rho_0) = T\exp(\int_0^t ds\mathcal{L}_s)\rho_0$, where T is the time ordering operator and the map $\Lambda_{t,0}$ is guaranteed to be CP if the underlying system-environment model is in a product state.

The master Eq. (5) generates maps that satisfy the semigroup property: $\Lambda_{t,s}$ being the map that evolves a state from time s to time t, then $\Lambda_{t,s} = \Lambda_{t,u}\Lambda_{u,s}$ for $t \geq u \geq s$. This means that the evolution can be split up into arbitrarily many segments that evolve the density matrix from one time to the next. However, complete positivity of $\Lambda_{t,0}$ does *not* necessarily guarantee that all intermediate maps $\Lambda_{s,u}$ are CP. When this is the case, all weights $\Gamma_k(t)$ are positive definite and (5) is of the Lindblad form.

If intermediate $\Lambda_{u,s}$ are not positivity preserving, not all quantum states map into quantum states, i.e., some quantum states map into operators with negative eigenvalues. $\Gamma_k(t)$ taking negative values captures an underlying system-environment model with meaningful entanglement. The reduced system state at an instant of time is no longer sufficient to describe the subsequent time evolution: one requires knowledge of the history of the system-environment interaction.

To illustrate this, we consider a qubit master equation employing four operators with their respective weight functions, i.e., $L_1 = \sigma_-$, $L_2 = \sigma_+$, $L_3 = \tau_-$ and $L_4 = \tau_+$ with $\sigma_\pm$ being the raising and lowering operators of σ_z and $\tau_\pm$ of σ_x, respectively. As weight factors we choose a

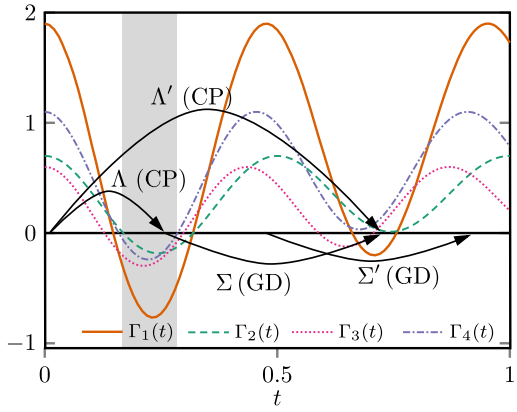

FIG. 3. Weight functions of the time local master equation (5). The rates are of the form $\Gamma_j(t) = a_j \exp(-t)[b_j - \sin^2(c_j \pi t)] - d_j$, with $a_2 = a_3 = 1$, $a_1 = 3$, and $a_4 = 1.5$; $b_1 = 4.5$, $b_2 = 3.5$, $b_3 = 1$, and $b_4 = 1.5$; $c_1 = 2$, $c_2 = 2$, $c_3 = 2.3$, and $c_4 = 2.2$, $d_1 = d_2 = 2.6$, and $d_3 = d_4 = 0.4$.

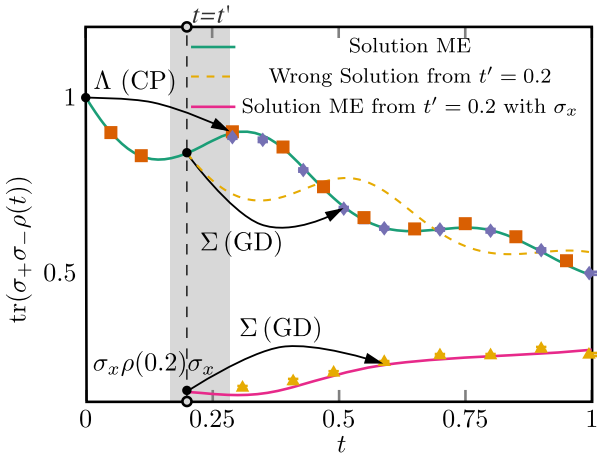

FIG. 4. Excited state population according to solutions of Eq. (5) (lines) and IBM simulations (symbols), for an initial state $\rho_0 = (1 + \sigma_z)/2$. In the shaded region all weights are negative, so the evolution starting from there is nonpositivity preserving. The dynamical map $\Lambda_t(0)$ is *CP*, while starting at a later time $t' = 0.2$, means the map $\Sigma \equiv \Lambda_{t,t'}$ is a general dynamical map. The (yellow) line shows the evolution of the state from time $t' = 0.2$ when the past interaction with the environment is not accounted for. The pink line (yellow triangles) displays the evolution from $t' = 0.20$ after applying a unitary transformation σ_x to the state.

typical non-Markovian model, which mimics resonance with an environmental mode [63]. Figure 3 displays these weight functions. The grey zone indicates the time region in which these weights are all negative. If the evolution of the density according to Eq. (5) starts in this time interval, for short times it will *not* be positivity preserving. Therefore, the solution of the master equation beginning from these times must be described within the above framework of general dynamical maps.

The excited state population according to Eq. (5) is shown in Fig. 4. The results obtained from the *CP* map $\Lambda_{t,0}[\rho_0]$ using $\rho_0 = (1 + \sigma_z)/2$ are displayed as a green full line obtained from a direct integration of (5), while those data points resulting from simulations on the IBM device (following the recipe outlined above) are squares. Starting at the intermediate time $t' = 0.2$ in the gray area of Fig. 3, diamonds display IBM simulations with the general dynamical map $\Sigma \equiv \Lambda_{t,t'}[\rho_{t'}]$. Since at t' all weight functions are negative definite, the solution (for short times, at least) is not *CP*. Consequently, when not accounting for the past interaction with the environment using $\Lambda_{t-t',0}[\rho_{t'}]$ (dashed yellow), the correct dynamics of Eq. (5) are not recovered.

Having access to the intermediate evolution maps starting from $t' > 0$ has a number of advantages. For example, we are able to evolve a state from 0 to t', perform a quantum operation on it, and then evolve it further with a completely bounded evolution. The (pink) full line in Fig. 4 displays this situation after applying the unitary transformation σ_x to the state at $t' = 0.2$, while the (yellow) triangles show the corresponding IBM simulations of the general dynamical map according to the new scheme.

Quantum state recovery.—An intriguing consequence of the new simulation method is that one can recover the initial state of an assumed Lindblad evolution obtained on a quantum device by implementing its time reversed master equation [64,65]. We consider a qubit weakly coupled to a thermal reservoir with forward time evolution $(d/dt)\rho_t = \mathcal{L}_t(\rho_t)$, where

$$\mathcal{L}_t(\rho_t) = -i\omega[\sigma_z/2, \rho_t] + \gamma e^{\beta\omega}\left(\sigma_-\rho\sigma_+ - \frac{1}{2}\{\sigma_+\sigma_-, \rho_t\}\right) + \gamma\left(\sigma_+\rho\sigma_- - \frac{1}{2}\{\sigma_-\sigma_+, \rho_t\}\right), \tag{6}$$

and its reversed evolution $(d/dt)\rho_t = -\mathcal{L}_t(\rho_t)$. Thus, evolving a state for a time t with Eq. (6) and then for a time $s \leq t$ with its time reversed version results in the state obtained by evolving with Eq. (6) for a time $t - s$. This is implemented on the IBM device according to Eq. (4).

In Fig. 1 data points for $t \leq t^*$ and various initial states reflect the thermalization dynamics of Eq. (6). At $t = t^*$, we recover earlier states in the dissipative time evolution. Note that the recovery is performed by mapping the state $\rho(t = t^*)$ directly to each recovered state with only one algorithm run per state.

Outlook.—We have shown that the class of general qubit dynamical maps can be straightforwardly simulated on quantum computing devices using just four extremal *CP* maps. For a given noise *CP* map of a single qubit, e.g., obtained according to [66], this allows us to revert it as demonstrated in Fig. 1, thus, performing genuine quantum error mitigation.

The decomposition of general dynamical maps in Eq. (4) holds for arbitrary (finite) dimensions. Taking it as a

starting point, the resulting multiqubit *CP* maps could be decomposed into single qubit maps. This could be achieved, for example, by using the circuit cutting scheme introduced in [67], and experimentally implemented in [68]. This scheme allows us to cut circuits up into smaller subcircuits at the price of having to realize these subcircuits for multiple input states.

We thank P. Muratore-Ginanneschi, M. Donvil, and J. Stockburger for valuable discussions. We thank G. McCaul for proofreading the manuscript. Financial support through the Ministery of Economy of the State of Baden-Württemberg within the Quantum Computing Competence Network Baden-Württemberg (project SiQuRe), the BMBF within QSens (QComp), and QSolid (BMBF) is gratefully acknowledged.

*brecht.donvil@uni-ulm.de

[1] I. M. Georgescu, S. Ashhab, and F. Nori, Rev. Mod. Phys. **86**, 153 (2014).
[2] S. Lloyd, Science **273**, 1073 (1996).
[3] D. W. Berry, G. Ahokas, R. Cleve, and B. C. Sanders, Commun. Math. Phys. **270**, 359 (2006).
[4] A. M. Childs, Commun. Math. Phys. **294**, 581 (2009).
[5] N. Wiebe, D. W. Berry, P. Høyer, and B. C. Sanders, J. Phys. A **44**, 445308 (2011).
[6] A. Rivas and S. F. Huelga, *Open Quantum System: An Introduction* (Springer, New York, 2012).
[7] A. Strathearn, P. Kirton, D. Kilda, J. Keeling, and B. W. Lovett, Nat. Commun. **9**, 3322 (2018).
[8] D. Suess, A. Eisfeld, and W. T. Strunz, Phys. Rev. Lett. **113**, 150403 (2014).
[9] J. Prior, A. W. Chin, S. F. Huelga, and M. B. Plenio, Phys. Rev. Lett. **105**, 050404 (2010).
[10] Y. Tanimura and R. Kubo, J. Phys. Soc. Jpn. **58**, 101 (1989).
[11] M. Xu, Y. Yan, Q. Shi, J. Ankerhold, and J. T. Stockburger, Phys. Rev. Lett. **129**, 230601 (2022).
[12] H. P. Breuer and F. Petruccione, *The Theory of Open Quantum Systems* (Clarendon Press, Oxford, 2002).
[13] G. Lindblad, Commun. Math. Phys. **48**, 119 (1976).
[14] V. Gorini, A. Kossakowski, and E. C. G. Sudarshan, J. Math. Phys. (N.Y.) **17**, 821 (1976).
[15] Á. Rivas, Phys. Rev. Lett. **124**, 160601 (2020).
[16] D. Bacon, A. M. Childs, I. L. Chuang, J. Kempe, D. W. Leung, and X. Zhou, Phys. Rev. A **64**, 062302 (2001).
[17] S. Lloyd and L. Viola, Phys. Rev. A **65**, 010101(R) (2001).
[18] H. Weimer, M. Müller, I. Lesanovsky, P. Zoller, and H. P. Büchler, Nat. Phys. **6**, 382 (2010).
[19] H. Wang, S. Ashhab, and F. Nori, Phys. Rev. A **83**, 062317 (2011).
[20] M. Kliesch, T. Barthel, C. Gogolin, M. Kastoryano, and J. Eisert, Phys. Rev. Lett. **107**, 120501 (2011).
[21] T. Barthel and M. Kliesch, Phys. Rev. Lett. **108**, 230504 (2012).
[22] G. McCaul, K. Jacobs, and D. I. Bondar, Phys. Rev. Res. **3**, 013017 (2021).
[23] J. D. Guimarães, J. Lim, M. I. Vasilevskiy, S. F. Huelga, and M. B. Plenio, arXiv.2302.14592.
[24] P. Schindler, M. Müller, D. Nigg, J. T. Barreiro, E. A. Martinez, M. Hennrich, T. Monz, S. Diehl, P. Zoller, and R. Blatt, Nat. Phys. **9**, 361 (2013).
[25] D.-S. Wang, D. W. Berry, M. C. de Oliveira, and B. C. Sanders, Phys. Rev. Lett. **111**, 130504 (2013).
[26] C. King and M. Ruskai, IEEE Trans. Inf. Theory **47**, 192 (2001).
[27] M. B. Ruskai, S. Szarek, and E. Werner, Linear Algebra Appl. **347**, 159 (2002).
[28] H. Lamm and S. Lawrence, Phys. Rev. Lett. **121**, 170501 (2018).
[29] Y. L. Jin-Fu Chen and H. Dong, Entropy **23**, 353 (2021).
[30] F. Ciccarello, S. Lorenzo, V. Giovannetti, and G. M. Palma, Phys. Rep. **954**, 1 (2022).
[31] M. Cattaneo, G. De Chiara, S. Maniscalco, R. Zambrini, and G. L. Giorgi, Phys. Rev. Lett. **126**, 130403 (2021).
[32] R. McCloskey and M. Paternostro, Phys. Rev. A **89**, 052120 (2014).
[33] S. Lorenzo, F. Ciccarello, and G. M. Palma, Phys. Rev. A **93**, 052111 (2016).
[34] S. Kretschmer, K. Luoma, and W. T. Strunz, Phys. Rev. A **94**, 012106 (2016).
[35] M. A. C. R. Guillermo García-Pérez and S. Maniscalco, npj Quantum Inf. **6**, 1 (2020).
[36] N. Cao, J. Lin, D. Kribs, Y.-T. Poon, B. Zeng, and R. Laflamme, arXiv:2111.02345.
[37] K. Temme, S. Bravyi, and J. M. Gambetta, Phys. Rev. Lett. **119**, 180509 (2017).
[38] S. Endo, S. C. Benjamin, and Y. Li, Phys. Rev. X **8**, 031027 (2018).
[39] J. Jiang, K. Wang, and X. Wang, Quantum **5**, 600 (2021).
[40] C. Song, J. Cui, H. Wang, J. Hao, H. Feng, and Y. Li, Sci. Adv. **5**, eaaw5686 (2019).
[41] S. Zhang, Y. Lu, K. Zhang, W. Chen, Y. Li, J.-N. Zhang, and K. Kim, Nat. Commun. **11**, 587 (2020).
[42] R. Feynman and F. Vernon, Ann. Phys. (N.Y.) **24**, 118 (1963).
[43] R. Karrlein and H. Grabert, Phys. Rev. E **55**, 153 (1997).
[44] M. W. Y. Tu and W.-M. Zhang, Phys. Rev. B **78**, 235311 (2008).
[45] G. M. G. McCaul, C. D. Lorenz, and L. Kantorovich, Phys. Rev. B **95**, 125124 (2017).
[46] B. Donvil, P. Muratore-Ginanneschi, and D. Golubev, Phys. Rev. B **102**, 245401 (2020).
[47] S. John and T. Quang, Phys. Rev. A **50**, 1764 (1994).
[48] N. Hashitsumae, F. Shibata, and M. Shingū, J. Stat. Phys. **17**, 155 (1977).
[49] R. Sweke, M. Sanz, I. Sinayskiy, F. Petruccione, and E. Solano, Phys. Rev. A **94**, 022317 (2016).
[50] See Supplemental Material at http://link.aps.org/supplemental/10.1103/PhysRevLett.131.110603 for a brief introduction to general dynamical maps, a summary of the results of [26,27] and a discussion of the error mitigation methods used in our simulations on the IBM quantum processors.
[51] B. Donvil and P. Muratore-Ginanneschi, New J. Phys. **25**, 053031 (2023).

[52] J. Han, W. Cai, L. Hu, X. Mu, Y. Ma, Y. Xu, W. Wang, H. Wang, Y. P. Song, C.-L. Zou, and L. Sun, Phys. Rev. Lett. **127**, 020504 (2021).
[53] V. Paulsen, *Completely Bounded Maps and Operator Algebras* (Cambridge University Press, Cambridge, England, 2003).
[54] E. C. G. Sudarshan and A. Shaji, J. Phys. A **36**, 5073 (2003).
[55] Actual data are obtained with the IBM quantum device in Ehningen, Germany.
[56] These recalibrations are done on a daily basis by the IBM staff, see https://quantum-computing.ibm.com/admin/docs/admin/calibration-jobs, accessed on the 6th of March 2023.
[57] R. Zwanzig, *Nonequilibrium Statistical Mechanics* (Oxford University Press, New York, 2001), p. 240.
[58] V. P. Vstovsky, Phys. Lett. **44A**, 283 (1973).
[59] H. Grabert, P. Talkner, and P. Hänggi, Z. Phys. B Condens. Matter **26**, 389 (1977).
[60] A. J. van Wonderen and K. Lendi, J. Stat. Phys. **80**, 273 (1995).
[61] E. Andersson, J. D. Cresser, and M. J. W. Hall, J. Mod. Opt. **54**, 1695 (2007).
[62] D. Chruściński and A. Kossakowski, Phys. Rev. Lett. **104**, 070406 (2010).
[63] H.-P. Breuer, E.-M. Laine, J. Piilo, and B. Vacchini, Rev. Mod. Phys. **88**, 021002 (2016).
[64] B. Donvil and P. Muratore-Ginanneschi, Nat. Commun. **13**, 4140 (2022).
[65] B. I. C. Donvil and P. M. Ginanneschi, New J. Phys. **25**, 053031 (2023).
[66] P. M. Mutter and G. Burkard, Phys. Rev. Lett. **128**, 236801 (2022).
[67] T. Peng, A. W. Harrow, M. Ozols, and X. Wu, Phys. Rev. Lett. **125**, 150504 (2020).
[68] C. Ying, B. Cheng, Y. Zhao, H.-L. Huang, Y.-N. Zhang, M. Gong, Y. Wu, S. Wang, F. Liang, J. Lin, Y. Xu, H. Deng, H. Rong, C.-Z. Peng, M.-H. Yung, X. Zhu, and J.-W. Pan, Phys. Rev. Lett. **130**, 110601 (2023).